BIOCHEMISTRY
including biophysical chemistry & molecular biology

Article

pubs.acs.org/biochemistry

Structural and Energetic Basis of Protein Kinetic Destabilization in Human Phosphoglycerate Kinase 1 Deficiency

Angel L. Pey,*[,†] Noel Mesa-Torres,[†] Laurent R. Chiarelli,[‡] and Giovanna Valentini[‡]

[†]Department of Physical Chemistry, Faculty of Sciences, University of Granada, Granada, Spain

[‡]Dipartimento di Biologia e Biotecnologie "L. Spallanzani", Università degli Studi di Pavia, Pavia, Italy

Supporting Information

ABSTRACT: Protein kinetic destabilization is a common feature of many human genetic diseases. Human phosphoglycerate kinase 1 (PGK1) deficiency is a rare genetic disease caused by mutations in the PGK1 protein, which often shows reduced kinetic stability. In this work, we have performed an in-depth characterization of the thermal stability of the wild type and four disease-causing mutants (I47N, L89P, E252A, and T378P) of human PGK1. PGK1 thermal denaturation is a process under kinetic control, and it is described well by a two-state irreversible denaturation model. Kinetic analysis of differential scanning calorimetry profiles shows that the disease-causing mutations decrease PGK1 kinetic stability from ∼5-fold (E252A) to ∼100000-fold (L89P) compared to that of wild-type PGK1, and in some cases, mutant enzymes are denatured on a time scale of a few minutes at physiological temperature. We show that changes in protein kinetic stability are associated with large differences in enthalpic and entropic contributions to denaturation free energy barriers. It is also shown that the denaturation transition state becomes more nativelike in terms of solvent exposure as the protein is destabilized by mutations (Hammond effect). Unfolding experiments with urea further suggest a scenario in which the thermodynamic stability of PGK1 at least partly determines its kinetic stability. ATP and ADP kinetically stabilize PGK1 enzymes, and kinetic stabilization is nucleotide- and mutant-selective. Overall, our data provide insight into the structural and energetic basis underlying the low kinetic stability displayed by some mutants causing human PGK1 deficiency, which may have important implications for the development of native state kinetic stabilizers for the treatment of this disease.

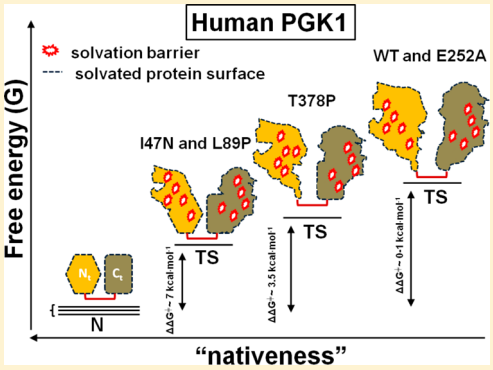

Phosphoglycerate kinase (PGK, EC 2.7.2.3) is an essential enzyme for all living organisms that catalyzes the reversible phosphotransfer from 1,3-bisphosphoglycerate to Mg-ADP to yield 3-phosphoglycerate (3-PG) and Mg-ATP.[1] Two human isoforms of PGK have been found, encoded by the *PGK-1* and *PGK-2* genes.[2,3] PGK1 and PGK2 are structurally and functionally similar enzymes, existing as ≈45 kDa monomers composed of two structural domains that are similar in size (see Figure 1A for the structure of human PGK1), sharing this two-domain structure with PGK proteins from multiple species (ref 4 and references cited therein).

Mutations in the *PGK-1* gene cause X-linked human PGK1 deficiency (OMIM entry 311800). PGK1 deficient patients show heterogeneous phenotypes including chronic nonspherocytic hemolytic anemia, neurological dysfunctions, and myopathies, even though the presence of all three types of clinical signs in the same patient is rare (reviewed in ref 5). This genetic disease has been found in ∼40 patients, and ∼20 different mutations have been shown to be disease-causing mutations. Approximately 80% of the mutations cause single-amino acid substitutions or small deletions.[5,6] The recent molecular characterization of most of the mutations described so far has shown that ∼75% of them reduced PGK1 kinetic stability, as seen by thermal inactivation kinetics, and ∼50% strongly lowered enzyme catalytic efficiency to less than 20% of that of the wild type (WT).[5,6] These functional studies have indicated that mutations mainly affecting PGK1 kinetic stability are linked to phenotypes, including hemolytic anemia and neurological symptoms, while those also causing strong catalytic perturbations are mostly related to myopathies with no hemolytic or neurological defects.[5,6] Despite these insightful studies, information about the structural and energetic basis of mutation-induced kinetic destabilization of PGK1 is still lacking.

Irreversible protein denaturation is described well for many proteins using a simple phenomenological two-state denaturation model:[7−9]

$$N \xrightarrow{k} F$$

where N and F represent the native and irreversible denatured state, respectively, and k is a strongly temperature dependent first-order rate constant. In this scenario, protein kinetic stability (as a given denaturation rate or half-life under certain experimental conditions) is determined by the height of the

Received: November 21, 2012
Revised: January 21, 2013
Published: January 21, 2013

   dx.doi.org/10.1021/bi301565m | *Biochemistry* 2013, 52, 1160−1170

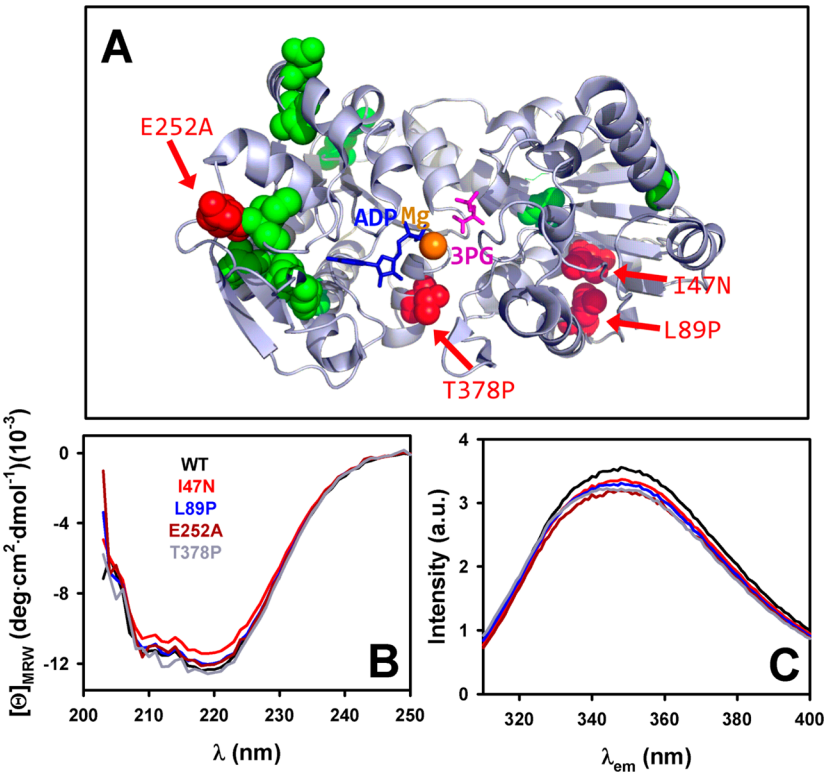

Figure 1. Structural and conformational properties of PGK1 enzymes. (A) Location of the amino acids affected by mutations of this study causing PGK1 deficiency (in red, PGK1 mutations studied here, while in green, other mutations known to be disease-causing) in a crystal structure of human PGK1 (Protein Data Bank entry 2WZC). Mg^{2+}, 3-PG, and ADP bound to PGK1 are also highlighted. (B and C) Far-UV circular dichroism (B) and tryptophan fluorescence (C) spectra. The color codes for panels B and C are the same. Spectra were recorded at 25 °C.

free energy barrier that the protein must cross from the native state to reach the rate-limiting denaturation step (i.e., the free energy difference between the native and denaturation transition states, $\Delta G^{\ddagger}$).[8] The irreversible thermal denaturation of different PGKs has been previously studied by differential scanning calorimetry (DSC), notably PGKs from yeast and pig (see an extensive compilation of these works in ref 10). In the absence of denaturants, PGK thermal denaturation is often found to be irreversible and displays a single calorimetric transition (despite the two-domain nature of the enzyme[10,11]).

The relevance of protein kinetic stability in many loss-of-function human genetic diseases is well-recognized.[8,12,13] Moreover, it has been proposed that kinetic stability is a "safety mechanism" developed by nature (through molecular evolution) to guarantee an adequate intracellular half-life for a protein to yield a physiologically relevant protein turnover and also to buffer to some extent the effect of destabilizing mutations.[8,14] Mutations may decrease protein kinetic stability by affecting either the (free) energy level of the native state or the denaturation transition state, thus reducing this free energy barrier. Detailed analyses of the mechanisms underlying mutational protein kinetic destabilization, as well as their structural and energetic basis, provide a solid framework for understanding disease mechanisms and developing new therapeutic strategies.[12,15−17] Actually, mechanistic information about mutational kinetic destabilization[15,18,19] paves the way for the rationale selection and development of native state kinetic stabilizers as therapeutic agents,[20] because those ligands preferentially binding to the native state will enhance kinetic stability to a larger extent (see ref 20 for an excellent example). However, large effects on the energy level of the denaturation transition state have also been shown to strongly affect protein kinetic stability (a remarkable example is the T119M trans-suppresor variant of transthyretin[20]).

In this work, we have performed a detailed characterization of the in vitro kinetic stability of human PGK1 WT and four mutants causing PGK1 deficiency (I47N, L89P, E252A, and T378P). The mutations were selected because a previous study showed that they differently affect PGK1 kinetic stability.[5] Our comparative study shows that these mutations decrease the PGK1 kinetic stability 5−100000-fold at physiological temperature. The decrease in the height of the denaturation free energy barrier correlates with large and highly compensated changes in activation enthalpies and entropies, likely due to large structural and energetic changes in the denaturation transition state as the kinetic stability decreases (analogue to the "Hammond effect" in protein folding of small proteins). To the best of our knowledge, we describe here for the first time this kind of Hammond effect in mutations causing a loss-of-function human genetic disease.

EXPERIMENTAL PROCEDURES

Expression and Purification of PGK1 Enzymes. Wild-type and mutant PGK1 proteins were expressed and purified essentially as previously described.[5] After the ion-exchange chromatography step, proteins were subjected to size exclusion chromatography on a 16/60 Superdex 200 column (GE Healthcare) to remove protein aggregates, and monomeric fractions were concentrated and buffer-exchanged with 20 mM HEPES, 200 mM NaCl, and 5 mM $MgCl_2$ (pH 7.4). Proteins were flash-frozen in liquid nitrogen and stored at −80 °C. Prolonged storage under these conditions (up to 6 months)

dx.doi.org/10.1021/bi301565m | Biochemistry 2013, 52, 1160−1170

prevented proteins from aggregation, which was routinely checked upon thawing for the absence of light scattering in absorption spectra, and unchanged far-UV CD and fluorescence spectra, size-exclusion chromatography profiles, and differential scanning calorimetry profiles. The protein concentration was measured using an ε_{280} of 27960 M^{-1} cm^{-1} based on the PGK1 primary sequence.

Spectroscopic Analyses. Spectroscopic analyses were performed in 20 mM HEPES, 200 mM NaCl, and 5 mM $MgCl_2$ (pH 7.4) at 25 °C. In all cases, the appropriate blanks were recorded and subtracted. Circular dichroism measurements were performed at 25 °C in a Jasco J-710 spectropolarimeter equipped with a Peltier temperature controller. Spectra were recorded at a scan rate of 50 nm/min, and four scans were registered and averaged, using 1 mm path-length cuvettes and 5−10 μM PGK1 protein. Tryptophan fluorescence spectra were recorded in a Cary Eclypse spectrofluorimeter (Varian), at a scan rate of 200 nm/min, and four scans were registered and averaged, using 3 mm path-length cuvettes and 3 μM PGK1 protein. The excitation wavelength was 295 nm, and excitation and emission slits were 5 nm.

Inactivation Experiments. To perform inactivation experiments, 180 μL of 20 mM HEPES, 200 mM NaCl, and 5 mM $MgCl_2$ (pH 7.4) was equilibrated at different temperatures (25−60 °C) for 10 min and 20 μL of 100 μM PGK1 proteins was diluted into the buffer and kept at the corresponding temperatures for 5 min. Then, 200 μL of 20 mM HEPES, 200 mM NaCl, 5 mM $MgCl_2$ (pH 7.4) buffer previously cooled to 4 °C was added, and the mixture was immediately chilled on ice and then flash-frozen in liquid nitrogen until activity measurements were taken. Activity measurements were performed in triplicate, using 0.01−0.04 μM PGK in a mixture containing 5 mM ATP, 5 mM 3-phosphoglycerate, 0.04 mg/mL GAPDH, and 0.24 mM NADH in 20 mM HEPES, 200 mM NaCl, and 5 mM $MgCl_2$ (pH 7.4). The consumption of NADH was measured at 340 nm in 1 cm cuvettes in a 8453 Agilent diode-array spectrophometer thermostated at 25 °C. One activity unit is defined as 1 μmol of NADH oxidized per minute.

Differential Scanning Calorimetry (DSC). Calorimetric studies were performed on a capillary VP-DSC differential scanning calorimeter (MicroCal, GE Healthcare) with a cell volume of 0.135 mL. Customarily, scans were performed at a rate of 1.5 °C/min in a temperature range of 5−70 °C using 10−20 μM PGK1 in 20 mM HEPES, 200 mM NaCl, and 5 mM $MgCl_2$ (pH 7.4), unless otherwise indicated. In some experiments, ATP or ADP was added to a final concentration of 3.2 mM (and their concentration was measured using an ε_{259} of 15400 M^{-1} cm^{-1}). To study the effect of urea on PGK1 denaturation, urea stock solutions were prepared in the buffer indicated above and the concentration of urea was determined by refractive index measurements.

DSC traces were modeled on the basis of a two-state irreversible model depicted by the following scheme:

$$N \xrightarrow{k} F$$

where N represents the native state, F represents the final state that cannot fold back to N under the given experimental conditions, and k is a first-order rate constant.[9] A detailed description of the models, fitting procedures, and consistency tests can be found elsewhere.[9,17,21] The rate constant k can be obtained from the experimental scans using the following expression:

$$k = \frac{\nu C_{p(\mathrm{exc})}}{\Delta H - \langle H \rangle} \tag{1}$$

where k is calculated using the excess heat capacity and the excess enthalpy at each temperature [$C_{p(\mathrm{exc})}$ and $\langle H \rangle$] and ν and ΔH are the scan rate and calorimetric enthalpy, respectively. The temperature dependence of the rate constants follows the Arrhenius equation:

$$k = A \exp\left(-\frac{E_a}{RT}\right) \tag{2}$$

where E_a is the activation energy and T is the absolute temperature in kelvin.

Calculation of Activation Thermodynamic Parameters. Mutational effects on the activation free energy ($\Delta\Delta G^{\ddagger}$), enthalpy ($\Delta\Delta H^{\ddagger}$), and entropy ($\Delta\Delta S^{\ddagger}$) were determined on the basis of the transition state theory as described in ref 21. The values of $\Delta\Delta H^{\ddagger}$ and $\Delta\Delta S^{\ddagger}$ were considered to be constant within the narrow range of the experiments and the relatively short extrapolations required for the most stable variants, as well as by the highly linear Arrhenius plots found in all cases. Mutational effects on activation energetic parameters were determined using eqs 3−5:

$$\Delta\Delta G^{\ddagger} = -RT \ln\left[\frac{k_{(37\,^{\circ}\mathrm{C})}(\mathrm{mut})}{k_{(37\,^{\circ}\mathrm{C})}(\mathrm{WT})}\right] \tag{3}$$

$$\Delta\Delta H^{\ddagger} = E_a(\mathrm{mut}) - E_a(\mathrm{WT}) \tag{4}$$

$$-T\Delta\Delta S^{\ddagger} = \Delta\Delta G^{\ddagger} - \Delta\Delta H^{\ddagger} \tag{5}$$

Contributions to Activation Energies from Unfolding and Solvation Barriers. Kinetic m values ($m^{\ddagger}$) were determined from the urea concentration dependence of the T_m and E_a values for each variant according to ref 21 using the following expression:

$$m^{\ddagger} = -\frac{E_a}{T_m}\left(\frac{dT_m}{d[\mathrm{urea}]}\right) - RT_m\left\{\frac{d\left[\ln\left(\frac{E_a}{RT_m^{\,2}}\right)\right]}{d[\mathrm{urea}]}\right\} \tag{6}$$

For each experimental scan rate, T_m and E_a values in the absence of urea are used, as well as the corresponding dT_m/d[urea] and d[ln($E_a/RT_m^{\,2}$)]/d[urea] values obtained from their dependence on urea concentration. The reported $m^{\ddagger}$ values are means ± standard deviation from three experimental scan rates.

The contributions of unfolding ($\Delta H_{\mathrm{UNF}}{}^{\ddagger}$) and solvation barriers (ΔH^*) to activation energies (≈activation enthalpies) were determined following the procedures described in refs 21 and 22. Briefly, $\Delta H_{\mathrm{UNF}}{}^{\ddagger}$ and ΔH^* were determined using the following expressions:

$$\Delta H_{\mathrm{UNF}}{}^{\ddagger} = \Delta H \frac{m^{\ddagger}}{m_{\mathrm{unf}}} \tag{7}$$

$$\Delta H^* = E_a - \Delta H_{\mathrm{UNF}}{}^{\ddagger} \tag{8}$$

where m_{unf} stands for the theoretical equilibrium m value.

The contributions of $\Delta H_{\mathrm{UNF}}{}^{\ddagger}$ and ΔH^* have been determined for each variant using four different methods to account for uncertainties in the different structural and energetic parametrizations: (i) different m_{unf}, calculated on

dx.doi.org/10.1021/bi301565m | Biochemistry 2013, 52, 1160−1170

the basis of either the number of residues of human PGK1 or the total change in accessible surface area (ΔASA) upon unfolding using a human PGK1 crystal structure [Protein Data Bank (PDB) entry 2WCZ] and a model based on the Gly-X-Gly tripeptide for the unfolded state,[22] or (ii) experimental ΔH for each variant or the theoretical ΔH values calculated at the T_m from the parametrization of Robertson and Murphy[23] based on the number of residues of PGK1. The structural changes associated with the transition between the native and transition states are calculated from the average values for $\Delta H_{UNF}^{\ddagger}$, and ΔH^*, which are estimated from the relation between these two parameters and ΔASA_{total} described by refs 23 and 21, respectively.

Urea-Induced Denaturation of WT PGK1. Concentrated urea stocks solutions were daily prepared in 20 mM HEPES, 200 mM NaCl, and 5 mM $MgCl_2$ (pH 7.4), and final urea concentrations were measured from their refractive indices. Equilibrium experiments were performed by incubation of protein solutions (2−5 μM) in the presence of different concentrations of urea in 20 mM HEPES, 200 mM NaCl, 5 mM $MgCl_2$, and 1 mM TCEP (pH 7.4) for at least 2 h at 25 °C, until a stable spectroscopic signal (circular dichroism or intrinsic fluorescence) was reached. Equilibrium unfolding curves were analyzed assuming a two-state unfolding model using the following expression:

$$S = \left\{S_N + m_N[\text{urea}] + [S_U + m_U[\text{urea}] \exp^{m_{N-U}([\text{urea}]-C_m)/RT}]\right\} \Big/ \left[1 + \exp^{m_{N-U}([\text{urea}]-C_m)/RT}\right] \quad (9)$$

where S is the spectroscopic signal, S_N and S_U are the signals corresponding to the native and unfolded states at 0 M urea, respectively, m_N and m_U are the linear dependencies of these signals on urea concentration, C_m is the urea concentration at $\Delta G_{N-U} = 0$, and m_{N-U} is the $-(\delta\Delta G/\delta[\text{urea}])$ at the C_m. ΔG_{N-U} is calculated at 0 M urea as the product $C_m m_{N-U}$ using the linear extrapolation method.[24]

Unfolding kinetics were monitored at 11−37 °C by following the changes in fluorescence at 350 nm upon excitation at 295 nm (10 nm slits). Urea solutions were prepared in 20 mM Hepes, 200 mM NaCl, and 5 mM $MgCl_2$ (pH 7.4) and equilibrated in 1 cm quartz cuvettes for 10 min, and a concentrated PGK1 solution was added to the cuvettes to a final concentration of 1−2 μM and mixed manually. The dead time of the measurement was registered (∼10 s) and taken into account in further analyses. The time dependence of the fluorescence change was described well in all cases by a simple exponential function, providing an apparent unfolding rate constant k. The dependence of k on urea concentration was assumed to be linear and analyzed using the following expression:

$$\ln k = \ln k_{0\,M} + \frac{m^{\ddagger}}{RT}[\text{urea}] \quad (10)$$

where $\ln k_{0\,M}$ is the natural logarithm of the rate constant extrapolated to the absence of urea and $m^{\ddagger}$ is the unfolding kinetic m value. The errors reported are those from fittings. The temperature dependence of $k_{0\,M}$ was analyzed according to the Arrhenius equation (eq 2).

RESULTS

Structural Location and Conformational Properties of PGK1 Enzymes in Solution. We have studied human PGK1 wild type (WT) and four mutants causing PGK1 deficiency, which were selected for the following reasons. (i) Mutations affect residues located either at the N-terminal or at the C-terminal domain of the human PGK1 structure (Figure 1A), and only two of them (I47N and L89P) are nearby in the crystal structure; the mutated residues show very different solvent accessibilities and predicted impacts on the native structure.[5] Their solvent accessibilities are 0% for I47, 4.8% for L89, 65.1% for E252, and 8.0% for T378. (ii) These five PGK1 enzymes are expected to show widely different kinetic stabilities.[5] Three of them showed similar thermal and kinetic stabilities as recently described via inactivation experiments (WT, E252A, and T378P), while the two remaining variants (I47N and L89P) displayed significantly reduced protein thermal and kinetic stability.[5] Therefore, these five PGK1 proteins are representative of different degrees of kinetic stabilities and locations on the native structure, and hence, they are suitable for providing insight into the energetic changes associated with the loss of kinetic stability in PGK1 deficiency.

All five PGK1 enzymes, purified to homogeneity upon recombinant expression in *Escherichia coli*, displayed similar hydrodynamic behavior as assessed by size exclusion chromatography (data not shown). Moreover, far-UV circular dichroism and intrinsic Trp fluorescence spectra of the mutant enzymes were very similar to that of WT PGK1 (Figure 1B,C), indicating that mutations did not perturb the overall structure of the native monomer to a large extent. Moreover, under the experimental conditions used, the specific activities of all PGK1 proteins at 25 °C (420 ± 15 units/mg for WT, 90 ± 6 units/mg for I47N, 260 ± 10 units/mg for L89P, 220 ± 23 units/mg for E252A, and 65 ± 6 units/mg for T378P) were in quite good agreement with our previous report under different experimental conditions.[5] At least three different protein preparations for each variant were obtained and used throughout this study, and most of the main results obtained in this work were checked to be independent of the protein batch used.

PGK1 Denaturation Follows a Simple Two-State Irreversible Model. Thermal denaturation of WT PGK1 monitored by DSC shows a single endothermic transition with a T_m of ∼53 °C (Figure 2). This transition is irreversible [no thermal effect is observed in a second up-scan (Figure 2A)] and scan rate-dependent (Figure 2B), indicating that PGK1 thermal denaturation is under kinetic control. Kinetically controlled protein denaturation is often described well by a simple two-state irreversible denaturation model:[8,25]

$$N \xrightarrow{k} F$$

Where the native state (N) is irreversibly converted to a final state (F) that cannot fold back, this conversion is characterized by a rate constant k. Protein aggregation is the likely origin of the irreversibility of thermal denaturation because samples withdrawn from the calorimeter upon completion of thermal transitions are evidently turbid. Analyses of WT and mutant PGK1 thermal denaturation using this simple model provide excellent fittings of the experimental thermal scans (Figures 2 and 3). Moreover, the values of the activation energy (E_a) using three of the methods proposed by Sanchez-Ruiz and co-workers[9] are consistent for each PGK1 enzyme (see Table 1 and Table S1 of the Supporting Information), and the observed

dx.doi.org/10.1021/bi301565m | *Biochemistry* 2013, 52, 1160−1170

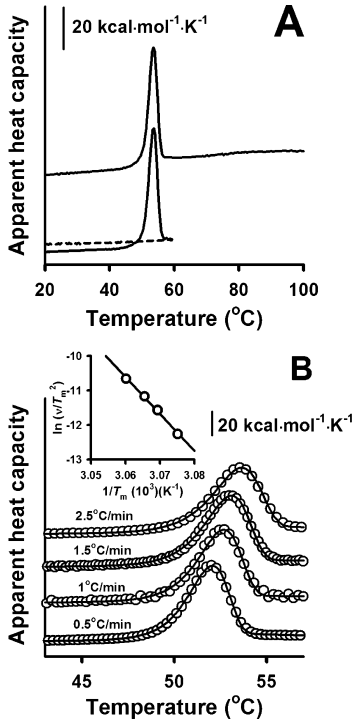

Figure 2. Thermal denaturation of WT PGK1 follows a two-state irreversible denaturation model. (A) Irreversibility of the thermal denaturation of WT PGK1. The top trace is from a single heating to 100 °C. The bottom traces is for a first scan up to 60 °C [a temperature at which the unfolding transition is completed (—)], then cooled to 10 °C, and rescanned (---). (B) Scan rate dependence of the denaturation of WT PGK1. The inset shows a plot of $\ln(\nu/RT_m^2)$ vs $1/T_m$, yielding a slope equal to $-E_a/R$.

uncertainties are well within the range reported for other protein systems analyzed by this simple two-state irreversible model.[22,26−29] Because all PGK1 enzymes show negligible effects of protein concentration on thermal denaturation profiles, denaturation kinetics is considered to be first-order

Table 1. Thermal Stability Parameters for Human PGK1 Enzymes Determined by DSC

	T_m (°C)[a]	E_a (kcal mol^{-1})[b]	ΔH (kcal mol^{-1})[c]	$t_{1/2(37\ °C)}$
WT	52.8 ± 0.2	191 ± 19	157 ± 18	≈3 years
I47N	44.6 ± 0.1	84 ± 6	66 ± 7	27 ± 1 min
L89P	43.0 ± 0.1	75 ± 3	60 ± 5	13 ± 1 min
E252A	52.1 ± 0.2	176 ± 12	130 ± 9	≈7 months
T378P	49.8 ± 0.4	135 ± 12	127 ± 9	3.9 ± 1.6 days

[a]Mean ± standard deviation (SD) from at least four independent experiments at a scan rate of 1.5 °C/min performed using two or three different protein batches. [b]Mean ± SD from three or four different scan rates. [c]Mean ± SD from at least eight different experiments.

[$\Delta T_m \leq 0.3$ °C in the 5−40 μM protein concentration range for each of the five PGK1 enzymes (data not shown)]. Overall, these data indicate that the analysis of thermal denaturation of all PGK1 enzymes is described well under our experimental conditions by a two-state irreversible denaturation model with first-order kinetics. We must also note that thermal transitions observed in DSC experiments agree well with the thermal inactivation scans performed (Figure 3A, inset), indicating that thermal denaturation analyses performed on the basis of DSC data coincide well with the relevant irreversible inactivation of PGK1 proteins.

Kinetic Stability Varies Widely among Disease-Causing Mutants. A wide range of denaturation temperatures (T_m values) is found for the PGK1 enzymes studied, ranging from ∼53 °C (WT) to ∼43 °C (L89P). Two additional parameters that characterize the thermal denaturation of PGK1 proteins are also shown to vary linearly according to the T_m of the PGK1 enzymes (Table 1 and Figure S1 of the Supporting Information). E_a values range from ∼190 (WT) to ∼75 kcal mol^{-1} (L89P), while ΔH values range from ∼160 (WT) to ∼60 kcal mol^{-1} (L89P). The strong temperature dependence of ΔH is not surprising if we consider that the denaturation change in heat capacity (ΔC_p) must be large for a protein of the size of PGK1. Structural and energetic correlations for protein

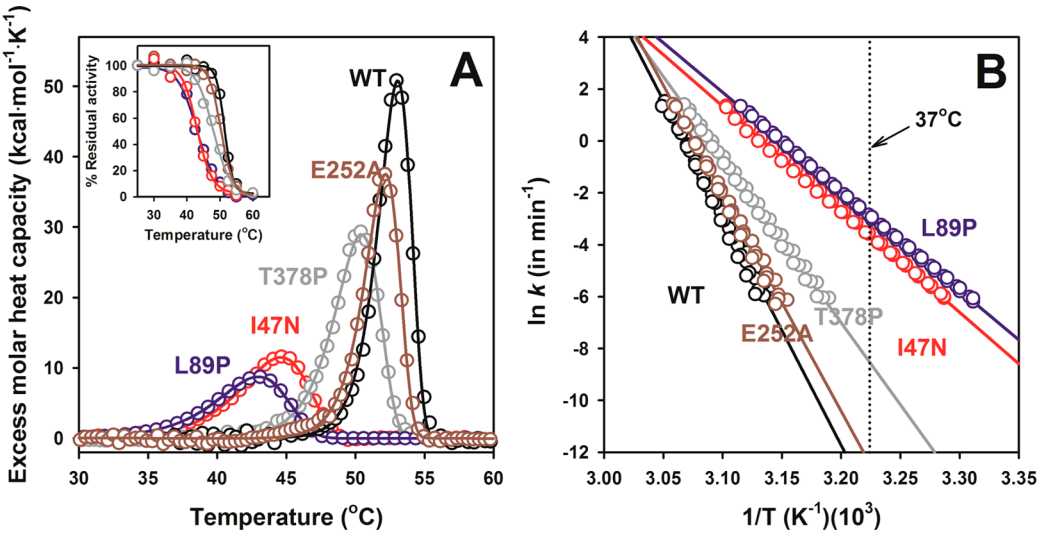

Figure 3. Kinetic stability of PGK1 enzymes monitored by DSC. (A) Thermal denaturation scans for all PGK1 enzymes (10−20 μM) performed at a rate of 1.5 °C/min; lines are best fits to a two-state denaturation model. The inset shows thermal inactivation scans after incubation for 10 min at different temperatures prior to activity measurements. (B) Arrhenius plots for PGK1 thermal denaturation. Experiments were performed at three or four scan rates (0.5−2.5 °C/min). The dotted vertical line in panel B indicates the physiological temperature.

dx.doi.org/10.1021/bi301565m | *Biochemistry* 2013, 52, 1160−1170

unfolding allow the estimation of theoretical ΔH and ΔC_p values for WT PGK1 of 250 kcal mol^{-1} (at 53 °C) and 5.8−7.0 kcal mol^{-1} K^{-1}, respectively.[23,30] These values agree reasonably well with those obtained experimentally for WT (ΔH = 157 ± 18 kcal mol^{-1}) and for the ΔC_p obtained for the five PGK1 enzymes [9.1 ± 0.8 kcal mol^{-1} K^{-1} (see Figure S1 of the Supporting Information)]. These results indicate that thermal denaturation and inactivation of PGK1 involve a large loss of tertiary structure and also suggest that all the enzymes are denatured to a similar extent, likely involving denaturation of both domains of human PGK1 (as recently proposed for other eukaryotic PGKs[10]).

Figure 3B shows the Arrhenius plots built for the PGK1 enzymes, which allow us to estimate the kinetic stabilities at 37 °C by either extrapolation (WT, E252A, and T378P) or interpolation (I47N and L89P). The corresponding half-lives are listed in Table 1. There is a remarkably wide range of kinetic stabilities (spanning more than 5 orders of magnitude) from the stable WT and E252A variant (half-lives in the range of months to years) to several mutants that are denatured in a few minutes (I47N and L89P) at physiological temperature, resulting from the intertwined decrease in T_m and E_a values found for the less stable PGK1 mutants.

Structural and Energetic Basis of the Different Kinetic Stabilities Found in PGK1 Mutants. The DSC analyses performed for all PGK1 enzymes show that activation energies (≈activation enthalpies) largely decrease according to the T_m value of the PGK1 enzyme (Table 1). A linear fit of E_a versus T_m values yields a slope of 10.2 ± 1.3 kcal mol^{-1} K^{-1} (Figure S1 of the Supporting Information), a value similar to that obtained for the denaturation ΔC_p (9.1 ± 0.8 kcal mol^{-1} K^{-1}). Provided that denaturation ΔC_p values are proportional to the change in the accessible surface area (ΔASA) between the native and unfolded states, a similar interpretation of the dependence of E_a on temperature would imply that the denaturation transition state (TS) is at least as solvent-exposed as the irreversibly denatured state. Alternatively, we may consider that the energetic balance in the denaturation transition state may differ from that found for native and unfolded states,[21,22,27] which would explain the large differences in E_a values found for the PGK1 enzymes without invoking such a largely unstructured and solvated denaturation TS.

An analysis of the enthalpic and entropic contributions to activation free energies shows that the significant differences in activation free energies observed among the PGK1 enzymes studied seem to arise from much larger mutational effects (of opposite sign) on the enthalpy and entropy contributions that largely cancel out (Figure 4A). It is unlikely that these mutational effects are mainly caused by gross changes in the native state structure of PGK1 mutants (Figure 1B,C). Alternatively, these effects may also be explained by the existence of a different energetic balance in the TS for denaturation of PGK1 enzymes.

Recent works have shown that this different energetic balance in the denaturation TS may involve the presence of contributions of "unfolding" (the native structure is disrupted, and a large fraction of the buried surface becomes solvated; this term is thus proportional to the difference in ASA between the native and denaturation TS) as well as from the so-called "solvation barriers" [i.e., networks of internal contacts that are broken in the denaturation TS but not yet solvated, therefore displaying energetic signatures different from those of the unfolding component (see refs 21 and 22 for a detailed discussion)]. Hence, the large dependence of E_a on the T_m values may involve the fact that the denaturation TS is largely unstructured and solvated (unfolding component), displays large solvation barriers, or shows significant contributions from both components.

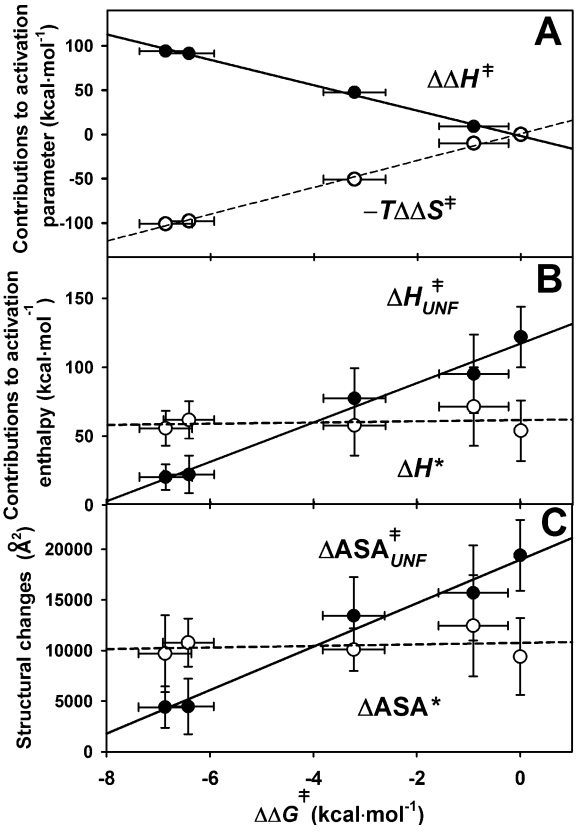

Figure 4. Energetic and structural consequences of PGK1 mutations on the denaturation free energy barrier. (A) Correlation between the changes in activation free energies ($\Delta\Delta G^{‡}$) and activation enthalpic ($\Delta\Delta H^{‡}$) and entropic ($-T\Delta\Delta S^{‡}$) contributions. (B and C) Energetic (B) and structural (C) contributions of unfolding ($\Delta H_{UNF}^{‡}$ and $\Delta ASA_{UNF}^{‡}$) and solvation barriers (ΔH* and ΔASA*) to activation energies for PGK1 variants. Lines are linear fits of the data in all panels.

To dissect the contributions of unfolding and solvation barriers, we have performed additional DSC experiments in the presence of nondenaturing urea solutions (Figure S2 of the Supporting Information) following the procedure described by Rodriguez-Larrea and co-workers,[21] which allows us to estimate both types of contributions separately. No significant deviations from a two-state irreversible denaturation model were observed in any of the variants (Table S2 of the Supporting Information). Both T_m and E_a values decreased in the presence of urea in all PGK1 enzymes (see Figure S2 of the Supporting Information for representative examples). These data allow us to determine the unfolding kinetic m values ($m^{‡}$), which provide an estimation of the difference in ASA between the native state and the denaturation TS (and allow us to estimate the unfolding contribution).[21] As shown in Table 2, the estimated $m^{‡}$ values largely vary among the PGK1 enzymes studied. These values are consistent with a fraction of the total ASA exposed to the solvent in the denaturation TS ranging from ∼0.6 (in the most stable enzymes, WT and E252A) to ∼0.2 (in the most unstable enzymes, I47N and L89P) (Table 2), suggesting that the solvent exposure of the TS decreases

dx.doi.org/10.1021/bi301565m | Biochemistry 2013, 52, 1160−1170

Table 2. Kinetic m Values ($m^{\ddagger}$) and Ratios of Kinetic to Equilibrium m Values ($m^{\ddagger}/m_{unf}$) for Thermal Denaturation of PGK1 Enzymes[a]

	$m^{\ddagger}$ (kcal mol^{-1} M^{-1})	$m^{\ddagger}/m_{unf}$	
		no. of residues[b]	ΔASA from crystal structure[c]
WT	2.95 ± 0.20	0.65 ± 0.04	0.50 ± 0.03
I47N	0.86 ± 0.16	0.19 ± 0.03	0.14 ± 0.03
L89P	0.86 ± 0.15	0.19 ± 0.03	0.14 ± 0.03
E252A	2.65 ± 0.28	0.58 ± 0.06	0.45 ± 0.05
T378P	2.21 ± 0.18	0.49 ± 0.04	0.37 ± 0.03

[a]Kinetic m values ($m^{\ddagger}$) are experimentally determined from the urea dependence of PGK1 thermal denaturation, while equilibrium m values (m_{unf}) are theoretical values determined for a protein of this size or based on the changes in ASA calculated from the crystal structure of human PGK1. [b]m_{unf} = 4.54 kcal mol^{-1} M^{-1}, based on ref 30 for a 417-residue monomer. [c]m_{unf} = 5.93 kcal mol^{-1} M^{-1}, based on ref 30 for a total ΔASA of 50528.4 Å^2 using the PGK1 crystal structure (PDB entry 2WZC) and the Gly-X-Gly model tripeptide for the unfolded state.[22]

according to the kinetic stability of the PGK1 enzyme. The $m^{\ddagger}$ values are then used to estimate the fraction of E_a or $\Delta H^{\ddagger}$ that corresponds to unfolding ($\Delta H_{UNF}{}^{\ddagger}$) and, by difference, provide an estimation of the contribution of solvation barriers (ΔH^*) contained in the activation enthalpies (Figure 4B). Despite this approach providing only approximate values for each kind of contribution, it is clear that the kinetic stability of PGK1 enzymes at physiological temperature correlates in energetic (Figure 4B) and structural (Figure 4C) terms with the solvent exposure of the denaturation TS (the solvent exposure of the TS decreases as the kinetic stability is reduced), while the contribution of solvation barriers is always significant but essentially unchanged among the PGK1 enzymes studied (Figure 4B,C).

Urea-Induced Unfolding of WT PGK1 Shows Low and Nearly Temperature-Independent $m^{\ddagger}$ Values. The largely different $m^{\ddagger}$ values observed between the PGK1 enzymes in the previous section raise the possibility that $m^{\ddagger}$ values are simply strongly temperature-dependent. To test this hypothesis, we have performed additional equilibrium and kinetic urea-induced denaturation experiments with WT PGK1. Incubations with high urea concentrations at 25 °C lead to a large decrease in the level of secondary structure (Figure 5A) and changes in the Trp emission fluorescence spectra (Figure 5B) consistent with extensive protein unfolding. These structural changes are fully reversible, as seen by the coincidence of the corresponding spectra at 1 M urea (nondenaturing) and those of the protein refolded from 5 to 1 M urea (data not shown). A single unfolding transition is observed for both structural probes, and

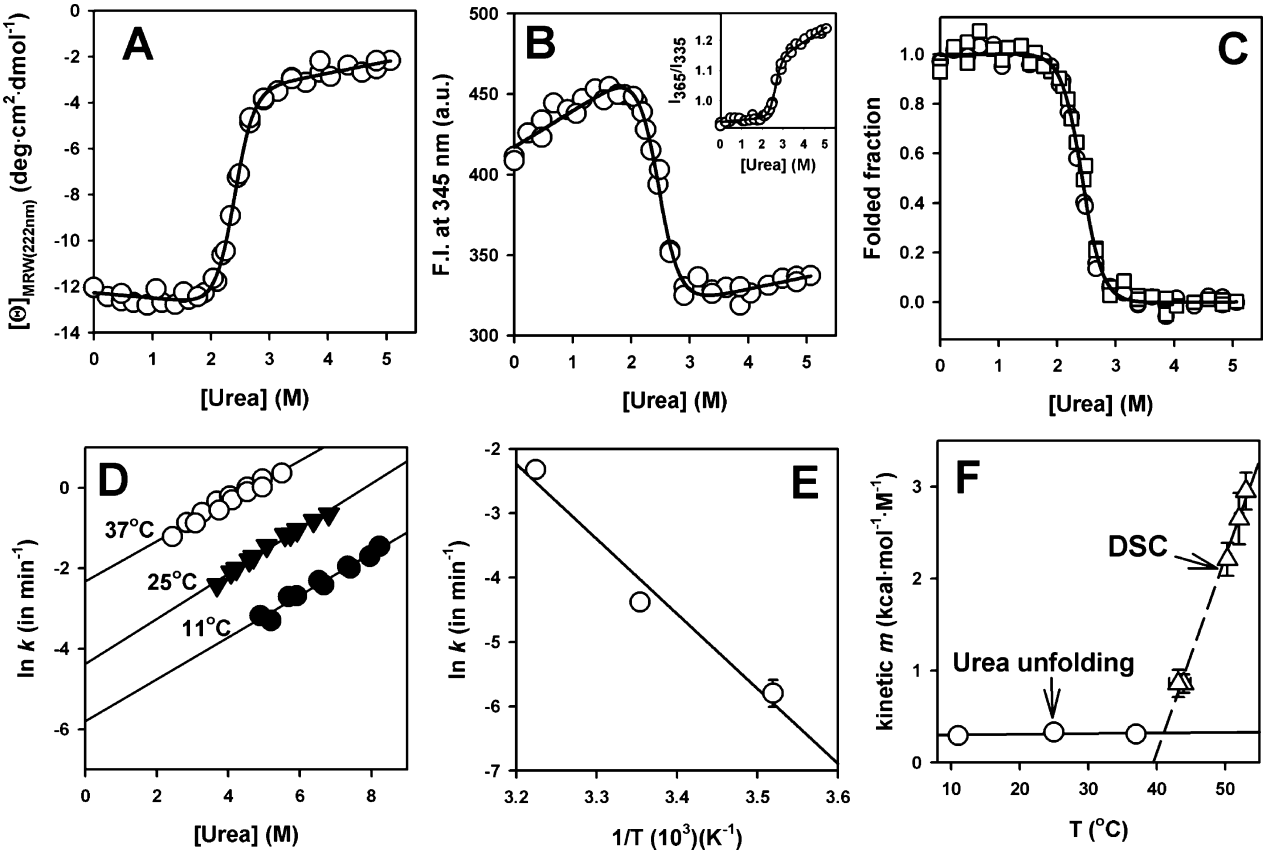

Figure 5. Urea-induced unfolding of WT PGK1. Equilibrium denaturation analyses monitored by far-UV CD (A) and Trp emission fluorescence (B) spectroscopy upon incubation of WT PGK1 with urea at 25 °C. The inset in panel B shows the ratio of fluorescence intensities at 365 and 335 nm reflecting the blue shift of fluorescence spectra upon unfolding. In panel C, we show the data from panels A (○) and B (□) upon subtraction of pre- and post-transition baselines. Solid lines in panels A–C are best fits to a two-state unfolding model (eq 9). Panel D shows the urea-induced unfolding rate constants determined by fluorescence spectroscopy at the indicated temperatures. Solid lines are best fits to eq 10, yielding the denaturation rate constants in the absence of denaturant (E) and $m^{\ddagger}$ values (○ in panel F). For comparison, we show the $m^{\ddagger}$ values determined by DSC for all PGK1 enzymes as a function of their average T_m value (△).

dx.doi.org/10.1021/bi301565m | Biochemistry 2013, 52, 1160–1170

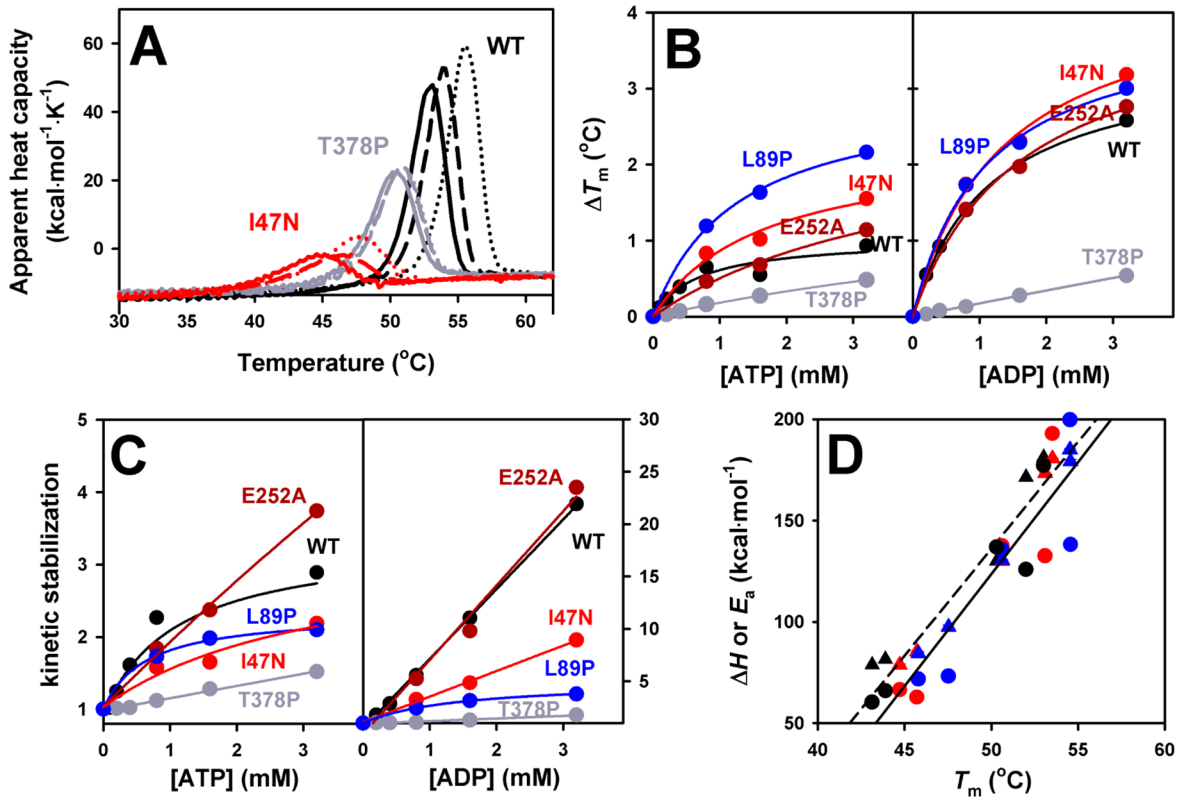

Figure 6. Thermal stabilization of PGK1 enzymes by nucleotides. (A) DSC scans of WT, T378P, and I47N in the absence (solid lines) or presence of ATP (dashed lines) or ADP (dotted lines) at 3.2 mM; the scan rate was 1.5 °C/min and the protein concentration 10−20 μM. (B) Nucleotide concentration dependence of thermal stabilization [change in T_m (ΔT_m)] for PGK1 enzymes. (C) Kinetic stabilization ($k_{\text{without nucleotide}}/k_{\text{with nucleotide}}$) of PGK1 enzymes by different nucleotide concentrations. (D) Dependence of ΔH (circles) and E_a (triangles) on nucleotide binding. Data are colored black (no nucleotide), red (average of all ATP concentrations), and blue (average of all ADP concentrations) for each PGK1 enzyme. Errors are smaller than the symbols.

they provide nearly identical unfolding profiles (Figure 5C), suggesting a two-state denaturation process. Simultaneous fitting of these curves to a two-state unfolding model yields the following values: C_m = 2.42 ± 0.01 M, and m_{unf} = 3.37 ± 0.21 kcal mol^{-1} M^{-1}. Using the linear extrapolation method,[24] a denaturation free energy change ($\Delta G_{N\leftrightarrow U}$) of 8.2 ± 0.5 kcal mol^{-1} is obtained, indicating a thermodynamic stability slightly lower than those reported for yeast and *E. coli* PGKs (9.3−9.7 kcal mol^{-1}).[31] We have further investigated urea-induced unfolding of WT PGK1 by performing unfolding kinetic experiments at three different temperatures. In all cases, a single exponential function described excellently the kinetic traces, and the corresponding amplitudes at different urea concentrations (at a fixed temperature) were nearly identical, indicating that the observed rate constants are dominated by the unfolding rates (data not shown). The unfolding branches obtained (Figure 5D) provide the following results. (i) Unfolding kinetics at 37 °C yield a denaturation half-life in the absence of denaturant of 7.1 ± 0.4 min, which is ∼5 orders of magnitude lower than the denaturation half-life for irreversible denaturation at the same temperature (∼3 years). (ii) The E_a for urea-induced denaturation kinetics is 23 ± 3 kcal mol^{-1} (Figure 5E), a value much lower than the E_a obtained for the WT or any of the PGK1 mutants studied (see Table 1). (iii) The $m^{\ddagger}$ values for the urea-induced unfolding are small (∼0.3 kcal mol^{-1} M^{-1}) compared to those obtained for the irreversible thermal denaturation (2.95 ± 0.20 kcal mol^{-1} M^{-1}) of WT PGK1, and $m^{\ddagger}$ values are nearly temperature-independent (Figure 5F).

The comparative kinetic analyses by DSC and urea-induced unfolding provide insightful details about the mechanism of irreversible denaturation of PGK1 enzymes. Consider the following simple mechanism:[7,32,33]

$$N \overset{K}{\leftrightarrow} U \overset{k}{\rightarrow} F$$

where N is the native state, U is an (ensemble) of unfolded state(s), F is the final irreversible denatured state, and the equilibrium (K) and kinetic constants (k) describe the N ↔ U and U → F steps, respectively. There are two limiting situations for this mechanism. (A) The irreversible U → F step is rate-limiting, and thus, the overall denaturation rate is determined by the product Kk. In this situation, the protein kinetic stability is at least partly determined by the thermodynamic stability of the protein (i.e., the value of K). (B) The irreversible U → F step is not rate-limiting, and hence, the overall denaturation rate is determined by the unfolding rate of the N → U step.[7] If we consider that the U state in this mechanism and the urea-induced unfolded state are similar, the lack of agreement between the denaturation rates, $m^{\ddagger}$ and E_a values found for WT PGK1 between thermal and urea denaturation may simply reflect the fact that the irreversible U → F step is rate-limiting (situation A), and thermodynamic stability may play a role in the kinetic stability of PGK1 variants at physiological temperature. Our results thus indicate that the different kinetic stabilities and the Hammond effect observed among the PGK1

dx.doi.org/10.1021/bi301565m | *Biochemistry* 2013, 52, 1160−1170

variants studied here are likely intrinsic properties of these proteins (possibly linked to their unfolding cooperativity) and not a simple temperature-dependent effect.

Native State Ligands Kinetically Stabilize PGK1 toward Irreversible Denaturation. We have tested the ability of two natural ligands of PGK1 (the ATP and ADP nucleotides) to kinetically stabilize the native state of the different PGK1 enzymes being studied, as previously shown for other eukaryotic PGKs.[10] As shown in panels A and B of Figure 6, both nucleotides were able to increase the T_m of all PGK1 enzymes in a concentration-dependent manner, but this effect was nucleotide- and mutant-selective. The average increase (ΔT_m) in the presence of 3.2 mM ATP or ADP was 1.4 ± 0.4 or 2.9 ± 0.3 °C, respectively, excluding the T378P variant that was less stabilized by the nucleotides (Figure 6B). This increase in thermal stability upon nucleotide binding was translated to kinetic stabilization of the native state, which was larger for ADP than for ATP [5−25-fold in the presence of 3.2 mM ADP vs 2−4-fold in the presence of 3.2 mM ATP, excluding again T378P (Figure 6C)]. The stronger kinetic stabilization provided by ADP might be partly explained by the higher affinity for this nucleotide (~11-fold higher than for ATP[34]). The weaker stabilization observed for T378P may be associated with a lower affinity of this variant for the nucleotides (5-fold higher K_M for ATP recently found for this mutant[5]). Visual inspection of the PGK1 crystal structure shows that residues 373−376 in helix 13 (where Thr378 is located) are in the proximity of the phosphate group of ADP, and the T378P mutation may severely perturb the local environment of helix 13, thus explaining the low binding affinity for nucleotides in this mutant. In all cases, the presence of the nucleotide did not produce significant deviations from the two-state model or any broadening of the denaturation transition (because of a possible specific stabilization of the nucleotide binding domain), as seen by the comparable values of E_a and ΔH obtained in the presence and absence of nucleotides (Figure 6D).

DISCUSSION

Recent studies have indicated that loss of function in human PGK1 deficiency may be caused in many cases by mutation-induced protein kinetic destabilization.[5,6,35] In this scenario, mutational effects on protein kinetic stability depend on their impact on the denaturation free energy barrier. In this work, we provide evidence supporting the idea that PGK1 kinetic destabilization by mutations causing PGK1 deficiency occurs through significant structural and energetic changes in the denaturation TS (Figure 7). While the most stable PGK1 enzymes (WT and E252A, with denaturation half-lives of ~3 years and ~7 months, respectively) show a more unstructured denaturation TS (i.e., with greater solvent exposure), as PGK1 kinetic stability is decreased upon mutation (to half-lives in the range of minutes), the denaturation TS becomes more compact (i.e., more protected from the solvent). These large differences in the structure and energetic balance of the denaturation TS among PGK1 variants with similar overall structure may appear striking. However, a similar situation has been recently described for TIM proteins from three different trypanosomatidae (*Trypanosoma cruzi*, *Trypanosoma brucei*, and *Leishmania mexicana*) with similar overall structures but widely divergent denaturation activation energetics (including largely different E_a values[22]). Actually, these authors suggested that the differences observed among these three TIM proteins might be the result of different levels of selection pressure associated with different

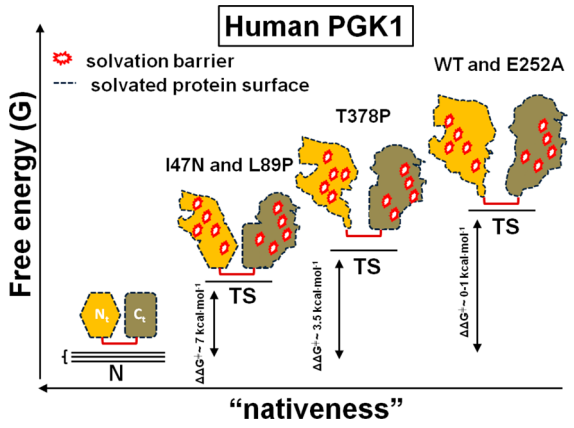

Figure 7. Pictorial representation of the mutational effects on the structure and energetics of PGK1 native and denaturation transition states, showing the proposed Hammond behavior for kinetically destabilizing mutations.

protein unfolding features (such as folding cooperativity[22]). Our results with these five human PGK1 enzymes suggest that WT PGK1 might have evolved to provide a high denaturation free energy barrier, including a large activation enthalpy through a largely unstructured TS, while the disease-causing mutations kinetically destabilize PGK1 at least partly by affecting the structure and energetics of the denaturation TS. We must note that the mutational effects described here for PGK1 denaturation structure and energetics seem to be uncoupled from their effects on PGK activity, which is expected because enzyme function is likely linked to the PGK1 native state ensemble (and not to the denaturation TS). The combination of urea-induced and thermally induced denaturation of PGK1 also indicates the irreversible U → F step is not rate-limiting, and thus, the reduced kinetic stability of PGK1 mutants is at least partly caused by a reduced thermodynamic stability for the N ↔ U step. It is also worth mentioning that yeast and pig muscle PGK proteins have also been shown to present relatively high activation energies (~120−130 kcal mol^{-1}) and similar T_m (~53−55 °C) compared to those of human WT PGK1,[10] suggesting that at least some of the energetic features providing kinetic stability to human WT PGK1 may be common to other eukaryotic PGKs. Thus, it is tempting to speculate that effects of mutations on the structure and energetics of the denaturation TS may lead to kinetic destabilization in other human loss-of-function genetic diseases. In this regard, a recent study of the kinetic destabilization of Uroporphyrinogen III synthase (UROIIIS[12]) by mutations causing congenital erythropoietic porphyria has shown that the most destabilizing mutations ($\Delta\Delta G^{\ddagger}$ = 1.4−3.6 kcal mol^{-1}) also display dramatic decreases in E_a values (lowering by 60−80% the value compared to that of WT, 70−90 kcal mol^{-1} in absolute terms), which may indicate a behavior for some disease-causing mutants of UROIIIS similar to that reported here for human PGK1 mutants.

The mutational effects on the structure and energetics of the denaturation TS reported by us here are large in quantitative terms. It is well-known that different challenges (mutagenesis, temperature, and denaturants) can move the position of the unfolding TS along a given reaction coordinate in small model proteins.[36−38] In some cases, such as barnase,[36] chymotrypsin inhibitor 2,[37] and domain 2 of gelsolin,[39] a decrease in the free energy gap between the native state and the denaturation TS

dx.doi.org/10.1021/bi301565m | *Biochemistry* 2013, 52, 1160−1170

may bring these states closer along a reaction coordinate (the so-called Hammond effect), a situation similar to the one described here for human PGK1-destabilizing mutations. It is also interesting to note that Hammond effects have been observed for mutations occurring in the hydrophobic core of barnase,[36] while the most destabilizing PGK1 mutations occur in residues with a solvent accessibility of <10% in the native state. The movements of the denaturation TS for PGK1 mutants are comparatively larger ($m^{\ddagger}/m_{unf}$ from ~0.6 to ~0.2) than those observed for smaller proteins (for instance, in the ~12 kDa barnase $m^{\ddagger}/m_{unf}$ changes from ~0.31 to ~0.13[36]), likely because of the larger kinetic destabilization induced by mutations in PGK1 ($\Delta\Delta G^{\ddagger}$ of up to approximately −7 kcal mol^{-1}) than, for instance, in barnase ($\Delta\Delta G^{\ddagger}$ of up to approximately −2 kcal mol^{-1}).[36] Interestingly, largely destabilizing mutations in UROIIIS ($\Delta\Delta G^{\ddagger}$ ~ −3.6 kcal mol^{-1}), a protein only slightly smaller than PGK1 (31 vs 45 kDa), are also associated with large decreases in E_a values (up to 90 kcal mol^{-1}),[12] which may also involve large structural changes in the denaturation TS. However, this proposal will remain speculative until additional information about the denaturation process of these mutants of UROIIIS is available.

In this report, we propose a link between kinetic stability and TS structural and energetic properties in PGK1-destabilizing mutations that may also provide insight into pharmacological treatments of human PGK1 deficiency targeting native state stability. Our data show that native state ligands (ADP and ATP) and naturally occurring osmolytes [trimethylamine *N*-oxide and sarcosine (unpublished observations)] selectively enhance native state kinetic stability of wild-type and mutant PGK1 proteins. However, because of the widely different structural and energetic properties of the TS found in different PGK1 mutants, development of these pharmacological therapies may include the evaluation of their possible effects on the TS (for instance, a ligand remaining bound to the TS), which will ultimately contribute to the net kinetic stabilization of the native state. In this regard, we have observed that native state ligands (ATP and ADP) kinetically stabilize PGK1 mutants in a mutant- and ligand-specific manner.

■ ASSOCIATED CONTENT

Supporting Information

Calorimetric analyses in the presence of urea as well as consistency tests for calorimetric data. This material is available free of charge via the Internet at http://pubs.acs.org.

■ AUTHOR INFORMATION

Corresponding Author

*Telephone: (+34) 958-240436. Fax: (+34) 958-272879. E-mail: angelpey@ugr.es.

Funding

This work was supported by Andalusian regional government Grant P11-CTS-07187 to A.L.P. A.L.P. is supported by a Ramón y Cajal research contract (RYC2009-04147). N.M.-T. is supported by a FPI predoctoral fellowship from the Spanish Ministry of Science and Innovation.

Notes

The authors declare no competing financial interest.

■ ACKNOWLEDGMENTS

We thank the three anonymous reviewers for insightful comments that helped to improve the manuscript.

■ ABBREVIATIONS

TS, transition state; PGK, phosphoglycerate kinase; DSC, differential scanning calorimetry; ASA, accessible surface area; $\Delta G^{\ddagger}$, activation free energy; $\Delta H^{\ddagger}$, activation enthalpy; $\Delta S^{\ddagger}$, activation entropy; E_a, activation energy; T_m, denaturation temperature; WT, wild-type.

■ REFERENCES

(1) Beutler, E. (2007) PGK deficiency. *Br. J. Haematol. 136*, 3−11.

(2) Willard, H. F., Goss, S. J., Holmes, M. T., and Munroe, D. L. (1985) Regional localization of the phosphoglycerate kinase gene and pseudogene on the human X chromosome and assignment of a related DNA sequence to chromosome 19. *Hum. Genet. 71*, 138−143.

(3) McCarrey, J. R., and Thomas, K. (1987) Human testis-specific PGK gene lacks introns and possesses characteristics of a processed gene. *Nature 326*, 501−505.

(4) Cliff, M. J., Bowler, M. W., Varga, A., Marston, J. P., Szabo, J., Hounslow, A. M., Baxter, N. J., Blackburn, G. M., Vas, M., and Waltho, J. P. (2010) Transition state analogue structures of human phosphoglycerate kinase establish the importance of charge balance in catalysis. *J. Am. Chem. Soc. 132*, 6507−6516.

(5) Chiarelli, L. R., Morera, S. M., Bianchi, P., Fermo, E., Zanella, A., Galizzi, A., and Valentini, G. (2012) Molecular insights on pathogenic effects of mutations causing phosphoglycerate kinase deficiency. *PLoS One 7*, e32065.

(6) Fermo, E., Bianchi, P., Chiarelli, L. R., Maggi, M., Mandara, G. M., Vercellati, C., Marcello, A. P., Barcellini, W., Cortelezzi, A., Valentini, G., and Zanella, A. (2012) A new variant of phosphoglycerate kinase deficiency (p.I371K) with multiple tissue involvement: Molecular and functional characterization. *Mol. Genet. Metab. 106*, 455−461.

(7) Plaza del Pino, I. M., Ibarra-Molero, B., and Sanchez-Ruiz, J. M. (2000) Lower kinetic limit to protein thermal stability: A proposal regarding protein stability in vivo and its relation with misfolding diseases. *Proteins 40*, 58−70.

(8) Sanchez-Ruiz, J. M. (2010) Protein kinetic stability. *Biophys. Chem. 148*, 1−15.

(9) Sanchez-Ruiz, J. M., Lopez-Lacomba, J. L., Cortijo, M., and Mateo, P. L. (1988) Differential scanning calorimetry of the irreversible thermal denaturation of thermolysin. *Biochemistry 27*, 1648−1652.

(10) Varga, A., Flachner, B., Graczer, E., Osvath, S., Szilagyi, A. N., and Vas, M. (2005) Correlation between conformational stability of the ternary enzyme-substrate complex and domain closure of 3-phosphoglycerate kinase. *FEBS J. 272*, 1867−1885.

(11) Galisteo, M. L., Mateo, P. L., and Sanchez-Ruiz, J. M. (1991) Kinetic study on the irreversible thermal denaturation of yeast phosphoglycerate kinase. *Biochemistry 30*, 2061−2066.

(12) Fortian, A., Castano, D., Ortega, G., Lain, A., Pons, M., and Millet, O. (2009) Uroporphyrinogen III synthase mutations related to congenital erythropoietic porphyria identify a key helix for protein stability. *Biochemistry 48*, 454−461.

(13) Martinez, A., Calvo, A. C., Teigen, K., and Pey, A. L. (2008) Rescuing proteins of low kinetic stability by chaperones and natural ligands phenylketonuria, a case study. *Prog. Mol. Biol. Transl. Sci. 83*, 89−134.

(14) Godoy-Ruiz, R., Ariza, F., Rodriguez-Larrea, D., Perez-Jimenez, R., Ibarra-Molero, B., and Sanchez-Ruiz, J. M. (2006) Natural selection for kinetic stability is a likely origin of correlations between mutational effects on protein energetics and frequencies of amino acid occurrences in sequence alignments. *J. Mol. Biol. 362*, 966−978.

(15) Johnson, S. M., Connelly, S., Fearns, C., Powers, E. T., and Kelly, J. W. (2012) The transthyretin amyloidoses: From delineating the molecular mechanism of aggregation linked to pathology to a regulatory-agency-approved drug. *J. Mol. Biol. 421*, 185−203.

(16) Nordlund, A., and Oliveberg, M. (2008) SOD1-associated ALS: A promising system for elucidating the origin of protein-misfolding disease. *HFSP J. 2*, 354−364.

(17) Pey, A. L., Salido, E., and Sanchez-Ruiz, J. M. (2011) Role of low native state kinetic stability and interaction of partially unfolded states with molecular chaperones in the mitochondrial protein mistargeting associated with primary hyperoxaluria. *Amino Acids 41*, 1233−1245.
(18) Hammarstrom, P., Schneider, F., and Kelly, J. W. (2001) Trans-suppression of misfolding in an amyloid disease. *Science 293*, 2459−2462.
(19) Jiang, X., Buxbaum, J. N., and Kelly, J. W. (2001) The V122I cardiomyopathy variant of transthyretin increases the velocity of rate-limiting tetramer dissociation, resulting in accelerated amyloidosis. *Proc. Natl. Acad. Sci. U.S.A. 98*, 14943−14948.
(20) Hammarstrom, P., Wiseman, R. L., Powers, E. T., and Kelly, J. W. (2003) Prevention of transthyretin amyloid disease by changing protein misfolding energetics. *Science 299*, 713−716.
(21) Rodriguez-Larrea, D., Minning, S., Borchert, T. V., and Sanchez-Ruiz, J. M. (2006) Role of solvation barriers in protein kinetic stability. *J. Mol. Biol. 360*, 715−724.
(22) Costas, M., Rodriguez-Larrea, D., De Maria, L., Borchert, T. V., Gomez-Puyou, A., and Sanchez-Ruiz, J. M. (2009) Between-species variation in the kinetic stability of TIM proteins linked to solvation-barrier free energies. *J. Mol. Biol. 385*, 924−937.
(23) Robertson, A. D., and Murphy, K. P. (1997) Protein Structure and the Energetics of Protein Stability. *Chem. Rev. 97*, 1251−1268.
(24) Greene, R. F., Jr., and Pace, C. N. (1974) Urea and guanidine hydrochloride denaturation of ribonuclease, lysozyme, α-chymotrypsin, and β-lactoglobulin. *J. Biol. Chem. 249*, 5388−5393.
(25) Sanchez-Ruiz, J. M. (1992) Theoretical analysis of Lumry-Eyring models in differential scanning calorimetry. *Biophys. J. 61*, 921−935.
(26) Pey, A. L., Majtan, T., Sanchez-Ruiz, J. M., and Kraus, J. P. (2012) Human cystathionine β-synthase (CBS) contains two classes of binding sites for S-adenosylmethionine (SAM): Complex regulation of CBS activity and stability by SAM. *Biochem. J. 449*, 109−121.
(27) Pey, A. L., and Martinez, A. (2009) Iron binding effects on the kinetic stability and unfolding energetics of a thermophilic phenylalanine hydroxylase from *Chloroflexus aurantiacus*. *J. Biol. Inorg. Chem. 14*, 521−531.
(28) Sot, B., Banuelos, S., Valpuesta, J. M., and Muga, A. (2003) GroEL stability and function. Contribution of the ionic interactions at the inter-ring contact sites. *J. Biol. Chem. 278*, 32083−32090.
(29) Vogl, T., Jatzke, C., Hinz, H. J., Benz, J., and Huber, R. (1997) Thermodynamic stability of annexin V E17G: Equilibrium parameters from an irreversible unfolding reaction. *Biochemistry 36*, 1657−1668.
(30) Myers, J. K., Pace, C. N., and Scholtz, J. M. (1995) Denaturant m values and heat capacity changes: Relation to changes in accessible surface areas of protein unfolding. *Protein Sci. 4*, 2138−2148.
(31) Young, T. A., Skordalakes, E., and Marqusee, S. (2007) Comparison of proteolytic susceptibility in phosphoglycerate kinases from yeast and *E. coli*: Modulation of conformational ensembles without altering structure or stability. *J. Mol. Biol. 368*, 1438−1447.
(32) Park, C., and Marqusee, S. (2004) Probing the high energy states in proteins by proteolysis. *J. Mol. Biol. 343*, 1467−1476.
(33) Tur-Arlandis, G., Rodriguez-Larrea, D., Ibarra-Molero, B., and Sanchez-Ruiz, J. M. (2010) Proteolytic scanning calorimetry: A novel methodology that probes the fundamental features of protein kinetic stability. *Biophys. J. 98*, L12−L14.
(34) Flachner, B., Varga, A., Szabo, J., Barna, L., Hajdu, I., Gyimesi, G., Zavodszky, P., and Vas, M. (2005) Substrate-assisted movement of the catalytic Lys 215 during domain closure: Site-directed mutagenesis studies of human 3-phosphoglycerate kinase. *Biochemistry 44*, 16853−16865.
(35) Ramirez-Bajo, M. J., Repiso, A., la Ossa, P. P., Banon-Maneus, E., de Atauri, P., Climent, F., Corrons, J. L., Cascante, M., and Carreras, J. (2011) Enzymatic and metabolic characterization of the phosphoglycerate kinase deficiency associated with chronic hemolytic anemia caused by the PGK-Barcelona mutation. *Blood Cells, Mol., Dis. 46*, 206−211.
(36) Matouschek, A., and Fersht, A. R. (1993) Application of physical organic chemistry to engineered mutants of proteins: Hammond postulate behavior in the transition state of protein folding. *Proc. Natl. Acad. Sci. U.S.A. 90*, 7814−7818.
(37) Matouschek, A., Otzen, D. E., Itzhaki, L. S., Jackson, S. E., and Fersht, A. R. (1995) Movement of the position of the transition state in protein folding. *Biochemistry 34*, 13656−13662.
(38) Matthews, J. M., and Fersht, A. R. (1995) Exploring the energy surface of protein folding by structure-reactivity relationships and engineered proteins: Observation of Hammond behavior for the gross structure of the transition state and anti-Hammond behavior for structural elements for unfolding/folding of barnase. *Biochemistry 34*, 6805−6814.
(39) Isaacson, R. L., Weeds, A. G., and Fersht, A. R. (1999) Equilibria and kinetics of folding of gelsolin domain 2 and mutants involved in familial amyloidosis-Finnish type. *Proc. Natl. Acad. Sci. U.S.A. 96*, 11247−11252.